THE JOURNAL OF BIOLOGICAL CHEMISTRY VOL. 280, NO. 45, pp. 37917–37923, November 11, 2005

Delineating a Ca^{2+} Binding Pocket within the Venus Flytrap Module of the Human Calcium-sensing Receptor*[S]

Received for publication, June 8, 2005, and in revised form, July 25, 2005 Published, JBC Papers in Press, September 7, 2005, DOI 10.1074/jbc.M506263200

Caroline Silve[‡1,2], Christophe Petrel[§1,3], Christine Leroy[‡], Henri Bruel[¶], Eric Mallet[‖], Didier Rognan[**], and Martial Ruat[§4]

*From [‡]INSERM, U426, Faculté de Médecine Xavier Bichat and IFR02, 16 Rue Henri Huchard, B.P. 416, F-75870 Paris, Université Paris 7, France, [§]Institut de Neurobiologie Alfred Fessard, IFR 2118 CNRS, Signal Transduction and Developmental Neuropharmacology, CNRS UPR9040, 1 Avenue de la Terrasse, 91198 Gif sur Yvette, France, [¶]Service de Médecine Néonatale, Groupe Hospitalier du Havre, 76083, Le Havre, France, [‖]Département de Pédiatrie, Hôpital Charles Nicolle, 76031 Rouen, France, and **Laboratoire de Pharmacochimie de la Communication Cellulaire, UMR7081 CNRS, 74 Route du Rhin, B.P. 24, F-67401 Illkirch, France*

The Ca^{2+}-sensing receptor (CaSR) belongs to the class III G-protein-coupled receptors (GPCRs), which include receptors for pheromones, amino acids, sweeteners, and the neurotransmitters glutamate and γ-aminobutyric acid (GABA). These receptors are characterized by a long extracellular amino-terminal domain called a Venus flytrap module (VFTM) containing the ligand binding pocket. To elucidate the molecular determinants implicated in Ca^{2+} recognition by the CaSR VFTM, we developed a homology model of the human CaSR VFTM from the x-ray structure of the metabotropic glutamate receptor type 1 (mGluR1), and a phylogenetic analysis of 14 class III GPCR VFTMs. We identified critical amino acids delineating a Ca^{2+} binding pocket predicted to be adjacent to, but distinct from, a cavity reminiscent of the binding site described for amino acids in mGluRs, GABA-B receptor, and GPRC6a. Most interestingly, these Ca^{2+}-contacting residues are well conserved within class III GPCR VFTMs. Our model was validated by mutational and functional analysis, including the characterization of activating and inactivating mutations affecting a single amino acid, Glu-297, located within the proposed Ca^{2+} binding pocket of the CaSR and associated with autosomal dominant hypocalcemia and familial hypocalciuric hypercalcemia, respectively, genetic diseases characterized by perturbations in Ca^{2+} homeostasis. Altogether, these data define a Ca^{2+} binding pocket within the CaSR VFTM that may be conserved in several other class III GPCRs, thereby providing a molecular basis for extracellular Ca^{2+} sensing by these receptors.

The class III G-protein-coupled receptors (GPCRs)[5] are activated by a variety of ligands, including calcium (Ca^{2+}), pheromones, L-amino acids, diverse natural sweeteners, and the major neurotransmitters glutamate and γ-aminobutyric acid (GABA). These receptors are characterized by a large amino-terminal extracellular domain reminiscent of bacterial periplasmic binding proteins. This domain is formed by two lobes (LB1 and LB2) separated by a cavity delineating the ligand-binding site and called a Venus flytrap module (VFTM) (1, 2). The crystal structure of the glutamate-bound form of the extracellular domain of the metabotropic glutamate receptor type 1 (mGluR1) revealed key residues located at the interface of LB1 and LB2 and that were involved in glutamate binding (3). Homology modeling of other class III GPCRs, including mGluRs and GABA-B type 1 (GBR1) receptors, the recently deorphanized receptor for basic amino acids (GPRC6a) and its goldfish relative, and the sweet taste receptors T1R1, T1R2, and T1R3, have helped identify the ligand binding pocket for these receptor ligands and the receptor activation process (4–7).

The Ca^{2+}-sensing receptor (CaSR) expressed in the parathyroid glands senses minor changes in ionized plasma Ca^{2+} and by controlling parathyroid hormone secretion is the major molecular determinant of Ca^{2+} homeostasis (8, 9). Initially cloned from the parathyroid glands (10), the CaSR has been subsequently isolated from various tissues, including kidney and brain, where it is proposed to mediate diverse physiologic effects in response to variations in extracellular Ca^{2+} (11–13). The cloning of the CaSR made it possible to demonstrate directly that the CaSR is activated not only by Ca^{2+} but also by Mg^{2+} and other divalent cations (10, 14–16). Molecules aimed at modulating the activity of the CaSR and acting at the level of the transmembrane domains have been characterized (17, 18). Indeed, targeting the parathyroid CaSR by a positive allosteric modulator has been proposed recently for the treatment of secondary hyperparathyroidism linked to renal disease (19), and antagonizing the CaSR activity might be of benefit for treating female osteoporosis (17).

Naturally occurring activating and inactivating CaSR mutations are responsible for autosomal dominant hypocalcemia (ADH) and familial hypocalciuric hypercalcemia (FHH), genetic diseases linked to perturbations in Ca^{2+} homeostasis (9, 20). The CaSR VFTM has been shown to contain the Ca^{2+}-binding site (21, 22). Among the 13 residues shown to be involved in glutamate binding to the mGluR1 VFTM, 6 are identical or conservatively substituted in the human CaSR (see supplemental Tables 3 and 4), and the analysis of variants produced by site-directed mutagenesis has shown that three of these residues impair Ca^{2+} activation when changed to alanine (21, 23). However, the Ca^{2+}-binding amino acids delineating the Ca^{2+} binding pocket within the CaSR VFTM have not been identified, nor is it known if this Ca^{2+} binding cavity is conserved within class III receptors.

In this study, we describe a homology model of the VFTM of the human CaSR built from the x-ray structure of the rat mGluR1 and a

* This work was supported in part by grants from INSERM (to C. S.). The costs of publication of this article were defrayed in part by the payment of page charges. This article must therefore be hereby marked "*advertisement*" in accordance with 18 U.S.C. Section 1734 solely to indicate this fact.

[S] The on-line version of this article (available at http://www.jbc.org) contains supplemental Tables 3–5.

[1] Both authors contributed equally to this work.

[2] Recipient of financial support from the Centre de Recherche Industriel et Technique.

[3] Supported by a grant from the Association pour la Recherche sur le Cancer.

[4] To whom correspondence should be addressed: CNRS UPR9040, 1 Avenue de la Terrasse, 91198 Gif sur Yvette, France. Tel.: 33-1-69-82-36-41; Fax: 33-1-69-82-36-39; E-mail: ruat@nbcm.cnrs-gif.fr.

[5] The abbreviations used are: GPCR, G-protein-coupled receptor; CaSR, Calcium sensing receptor; GABA, γ-aminobutyric acid; VFTM, Venus flytrap module, mGluR1, metabotropic glutamate receptor type 1; LB, lobe; GBR1, GABA-B receptor type 1; T1R1, T1R2, T1R3, sweet taste receptors type 1, type 2, type 3; ADH, autosomal dominant hypocalcemia; FHH, familial hypocalciuric hypercalcemia; IP, inositol phosphate; WT, wild type.

phylogenetic analysis of the ligand binding pocket of class III GPCRs. This model, which predicts the residues contributing to Ca^{2+} recognition, indicates that Ca^{2+} does not interact with amino acids homologous to those delineating the glutamate binding cavity but to a site adjacent to this cavity. We used mutational analysis, including the description and characterization of a novel mutation associated with ADH, and data from the literature to validate our model. In addition, our data are consistent with the presence of a conserved Ca^{2+} binding pocket within the VFTM of other class III GPCRs, adding a molecular basis for the previously observed effects of extracellular Ca^{2+} on the action of these receptors.

EXPERIMENTAL PROCEDURES

Identification of E297D Mutation in the CaSR Associated with ADH—Genomic DNA from the proband and family members was isolated from peripheral leukocytes using standard methods. CaSR exons 2–7 (proband) and exon 4 (all family members) and the corresponding intron-exon junctions were amplified using intronic primers (sequences available on request). PCR-amplified products were sequenced as described (24).

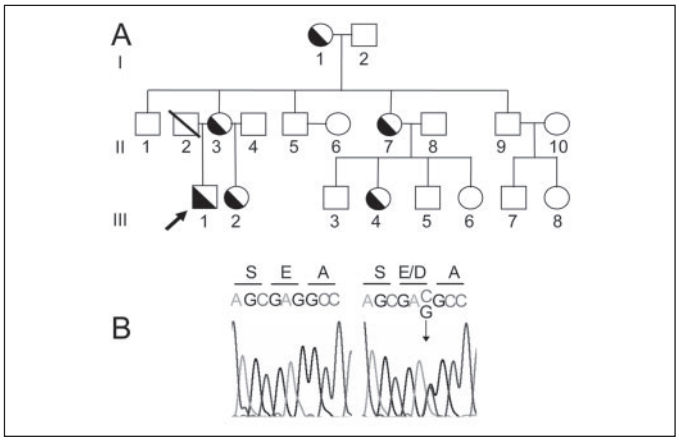

FIGURE 1. **Identification of the E297D activating mutation in the CaSR gene in patients affected with ADH.** *A,* three-generation pedigree of the family affected with ADH because of a heterozygous E297D mutation in the CaSR gene. *B,* DNA sequence of the CaSR gene. The index case (*black arrow*) and affected members harbored a heterozygous G to C substitution at codon 297, which would result in substitution of aspartic acid for glutamic acid (E297D) in the CaSR VFTM.

Site-directed Mutagenesis—Wild-type (WT) cDNA encoding the human CaSR inserted in pcDNA3.1/Hygro plasmid was a kind gift of E. F. Nemeth and P. Jacobson (NPS Pharmaceuticals Inc., Salt Lake City, UT). Missense mutations were introduced in the WT cDNA construct using the Quick Change Site-directed Mutagenesis kit (Stratagene) and were confirmed by complete sequencing of cDNA inserts (Genome Express, Meylan, France) (oligonucleotide sequences available on request).

Cell Culture, Transient Transfection, and Western Blot Analysis—Experiments were performed in HEK293 cells. Techniques used for cell culture, transient transfection by electroporation, and the detection of WT and mutant CaSRs expression by Western blot analysis have been described (25).

[^{3}H]IP Formation—Cells were cultured in the presence of 0.5 μCi/well myo-[^{3}H]inositol (Amersham Biosciences) for 20 h. The measurement of [^{3}H]IP accumulation was performed in freshly prepared buffer (125 mM NaCl; 4.0 mM KCl; 0.5 mM $MgCl_2$; 20 mM Hepes; 0.1% D-glucose, pH 7.4) containing the indicated $CaCl_2$ concentration (25). Two to five independent experiments were performed in duplicate or triplicate using the same conditions. The data were fitted to a sigmoid dose-response curve to determine EC_{50} values by using the GraphPAD Prism. Values for each curve were normalized to the maximal activation of each receptor, obtained by stimulation with 20 mM Ca^{2+}. Significance was assayed by Excel 2000 Student's *t* test.

Homology Modeling of the Amino-terminal Domain of the Calcium-sensing Receptor—A multiple alignment of 14 class III GPCR extracellular domains (shown in supplemental Table 3) was obtained with the T-Coffee program (26) Homology modeling of the human CaSR was performed with the SYBYL6.91 package (TRIPOS Associates Inc., St. Louis, MO) starting from monomer A of the mGluR1 x-ray structure (Protein Data Bank code 1ewk) (3). The insertion of residues in loops between helix A and strand B, helix B and strand D, and helix L and helix M (3) was accommodated by a knowledge-based loop search procedure as described previously (27). Further energy refinement of the model was achieved by a standard minimization protocol using the AMBER 8 program (University of California, San Francisco). Mapping of the Ca^{2+}-binding site was performed using the GRID version 20 software (28) using a Ca^{2+} probe and standard settings for the grid definition. The most energetically favored location of the calcium ion was then used to minimize (by 1,000 steps of steepest descent followed by 1,000 steps of conjugate gradient refinement) the receptor model in the pres-

TABLE ONE

Alignment of 19 amino acids lining the orthosteric binding site of 14 human class III GPCRs

Here we report a natural activating mutation affecting Glu-297 (boldface) associated with ADH.

Receptor	Binding site residues																		
mGluR1	Y74	R78	W110	S164	S165	S166	S186	T188	D208	Q211	Y236	F290	E292	G293	S317	D318	G319	R323	K409
mGluR2	R57	R61	S93	Y144	S145	D146	A166	T168	D188	Q191	Y226	F269	R271	S272	S294	D295	G296	L300	K377
mGluR3	R67	R71	S103	Y153	S154	S155	A175	T177	D197	Q200	Y225	F278	R280	S281	S303	D304	G305	Q309	K392
mGluR4	K74	R78	S110	G158	S159	S160	A180	T182	D202	Q205	Y230	F284	N286	E287	S311	D312	S313	K317	K405
mGluR5	Y64	R68	W100	S151	S152	S153	S173	T175	D195	Q198	Y223	F277	E279	G280	S304	D305	G306	R310	K396
mGluR6	Q64	R68	S100	A153	S154	S155	A175	T177	D197	Q200	Y225	F279	N281	E282	S306	D307	S308	K312	K400
mGluR7	N64	R78	S110	G158	S159	S160	A180	T182	D202	Q205	Y230	F286	N288	D289	S313	D314	S315	K319	K407
mGluR8	K71	R75	S107	A155	S156	S160	A177	T179	D199	Q202	Y227	F281	N283	E284	S308	D309	S310	K314	R401
GPRC6a	S69	Q73	T104	Y148	S149	E150	E170	T172	D192	Q195	Y220	F277	R279	Q280	S302	D303	N304	A308	E408
GBR1	G184	C188	D221	C246	S247	S248	G268	S270	A290	H293	V318	L365	Y367	E368	A397	D398	N399	I403	E466
CaSR	R66	W70	N102	G146	S147	G148	A168	S170	D190	Q193	Y218	F270	S272	G273	S296	**E297**	A298	S302	H413
T1R1	H71	L75	S107	S148	T149	N150	A170	S172	D192	Q195	Y220	F274	S226	R227	S300	E301	A302	S306	M383
T1R2	I67	L71	Y103	N143	S144	E145	S165	I167	A187	H190	Y215	F275	P277	D278	S301	E302	S303	D307	E382
T1R3	N68	W72	S104	S146	S147	E148	G168	S170	D190	Q193	Y218	F274	S276	V277	S300	E301	A302	S306	H387

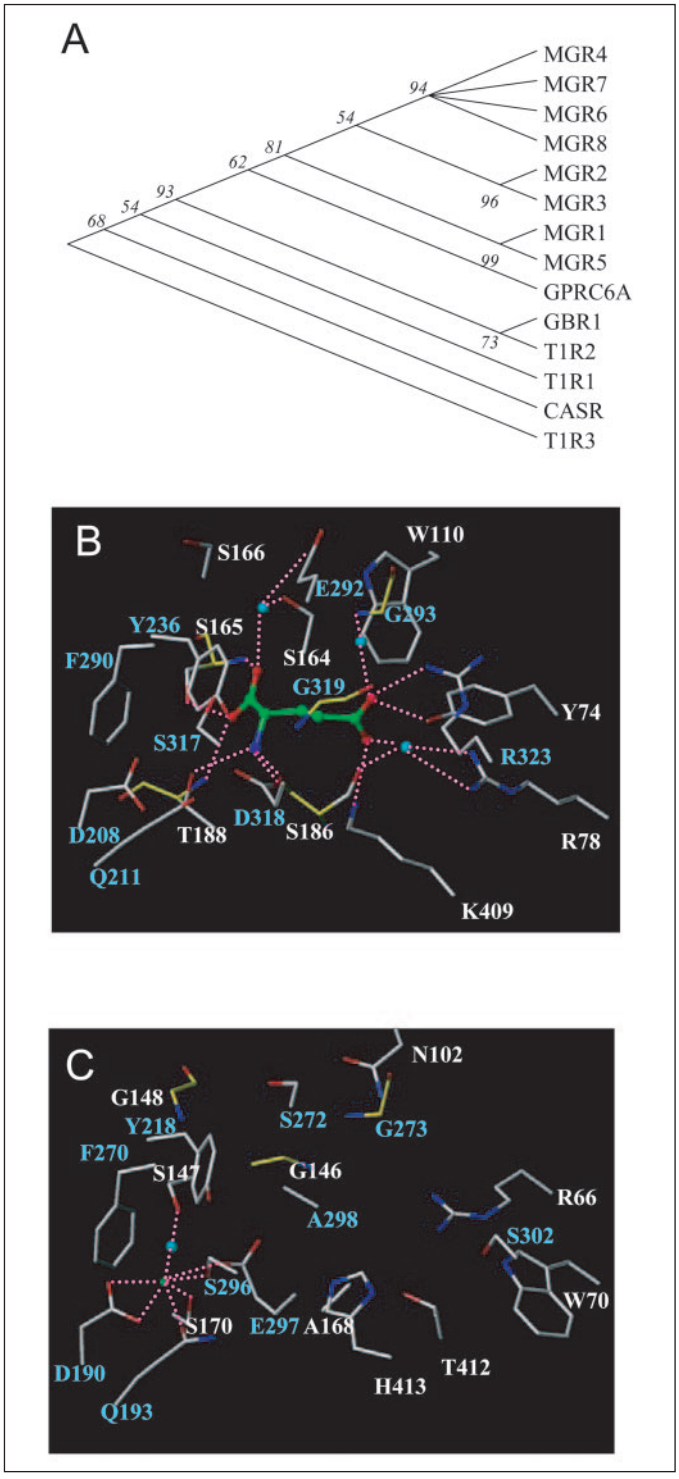

FIGURE 2. **Phylogenetic tree of class III GPCR ligand binding pocket (*A*) and molecular modeling of the human mGluR1 (*B*) and CaSR (*C*) ligand binding pockets.** *A,* neighbor-joining tree of human class III GPCRs. The 19 residues lining the binding pocket of human class III GPCRs (supplemental Table 4) were extracted to calculate a distance matrix with the MEGA2 software (29). A neighbor-joining tree was calculated out of 100 bootstrap replicas using the γ correction for estimating pairwise protein distances. Bootstrap values are indicated in *italics. B* and *C,* ligand binding pocket of mGluR1 (*B*) and CaSR (*C*). Receptor atoms are shown as *capped sticks*, whereas ligand atoms are shown in *ball* and *sticks* (*white*, receptor carbon atom; *green*, L-glutamate carbon atoms; *red*, oxygen; *blue*, nitrogen). Main chain atoms of the receptor participating in H-bonds to the ligands are displayed in *yellow*. Residues from the ligand binding domains 1 and 2 (LB1 and LB2) are labeled at the C-α atoms in *white* and *cyan*, respectively. Water molecules mediating ligand binding are displayed as *cyan balls. Pink dashed lines* indicate electrostatic (H-bonds, ion coordination) intermolecular interactions. *B,* the amino-terminal mGluR1-binding site residues were taken from the glutamate-liganded x-ray structure of rat mGluR1 (Protein Data Bank code 1ewk) (3). *C,* CaSR Ca^{2+}-binding site was modeled from the rat mGluR1 structure. Coordinates of the calcium ion are displayed by a *green ball. A water molecule (cyan ball)* completes the pentagonal bispyramidal coordination of the calcium ion.

ence of Ca^{2+} and within a box of 23,844 TIP3P water molecules, placed automatically with the leap module of AMBER 8.0.

Neighbor-joining Tree—19 residues lining the binding pocket of glutamate in the mGluR1 structure (3) were extracted from 14 human class III GPCRs, concatenated into ungapped sequences, and were used to calculate a distance matrix with the MEGA2 software (29). A neighbor-joining tree was calculated out of 100 bootstrap replicas using the γ correction for estimating pairwise protein distances.

RESULTS

Identification of E297D Mutation in the CaSR Associated with ADH—The three generation pedigree of the family affected with ADH is shown in Fig. 1*A*. The index case was diagnosed during the 1st month of life because of severe hypocalcemic symptoms requiring calcium infusion. Biochemical features of the proband and family members at the time of diagnosis of hypocalcemia and identification of the activating mutation in the CaSR are shown in supplemental Table 5.

Direct sequence analysis of the PCR-amplified CaSR exons led to the identification of a heterozygous G to C nucleotide substitution in exon 4 of the CaSR gene at position 889 of the CaSR cDNA sequence (Fig. 1*B*). This base change resulted in the substitution of glutamate for aspartate at position 297 (E297D) located in the extracellular domain. The E297D mutation was present in all affected family members and absent in others (data not shown). Most interestingly, a missense E297K mutation has been identified in subjects with FHH (30, 31).

Phylogenetic Tree of the Ligand Binding Pocket of Family 3 GPCRs—The Glu-297 residue is structurally homologous to an aspartate residue conserved in all mGluRs that is located within the mGluR VFTM (TABLE ONE and supplemental Table 4) and has been implicated in ligand binding and receptor activation (3, 4). This suggests that Glu-297 is part of the Ca^{2+} binding pocket of the CaSR. In an attempt to delineate the putative ligand binding pocket of this receptor, we first constructed a phylogenetic tree for 14 human class III GPCRs based on 19 residues (TABLE ONE) lining the glutamate binding cavity identified in the mGluR1 structure (3). This phylogenetic tree indicates that the CaSR-binding site is not closely related to that of any other receptors (Fig. 2*A*), including the GPRC6a receptor recognizing basic amino acids (7). This latter receptor shows the highest overall homology with the CaSR (TABLE ONE and supplemental Table 4), but its ligand-binding site segregates more closely with that of the mGluRs (Fig. 2*A*). Most interestingly, the binding sites of the CaSR, T1R1, T1R2, T1R3, and GBR1 form a cluster distinct from that of mGluRs (Fig. 2*A*).

Molecular Modeling of the Ca^{2+}-binding Site of the CaSR—We next developed a homology model of the extracellular domain of the human CaSR built from the x-ray structure of the mGluR1 and according to a multiple alignment of the above-mentioned receptor sequences (supplemental Table 4). Comparison of the molecular models of the human mGluR1 and CaSR ligand binding pockets shows that the overall three-dimensional structure of the CaSR amino-terminal tail is very similar to the x-ray structure of the rat mGluR1 described by Kunishima *et al.* (3) (Fig. 2, *B* and *C*). Only three insertions in loop regions occur (see "Experimental Procedures"). The multiple sequence alignment used to thread the CaSR coordinates onto the mGluR1 structure (TABLE ONE and supplemental Table 4) shows only a single difference with that published (3) and occurs just before the beginning of helix M at Lys-409, which is a glutamate-anchoring residue. We propose a shorter insertion

TABLE TWO

Amino acids lining the putative Ca^{2+}-binding site of human class III GPCRs

Conserved and conservatively substituted amino acids are indicated in boldface and underlined text, respectively.

Receptor	Binding residues							
mGluR1	**S165**	T188	**D208**	**Q211**	**Y236**	**F290**	**S317**	D318
mGluR2	**S145**	T168	**D188**	**Q191**	**Y226**	**F269**	**S294**	D295
mGluR3	**S154**	T177	**D197**	**Q200**	**Y225**	**F278**	**S303**	D304
mGluR4	**S159**	T182	**D202**	**Q205**	**Y230**	**F284**	**S311**	D312
mGluR5	**S152**	T175	**D195**	**Q198**	**Y223**	**F277**	**S304**	D305
mGluR6	**S154**	T177	**D197**	**Q200**	**Y225**	**F279**	**S306**	D307
mGluR7	**S159**	T182	**D202**	**Q205**	**Y230**	**F286**	**S313**	D314
mGluR8	**S156**	T179	**D199**	**Q202**	**Y227**	**F281**	**S308**	D309
GPRC6a	**S149**	T172	**D192**	**Q195**	**Y220**	**F277**	**S302**	D303
GBR1	**S247**	**S270**	A290	H293	V318	L365	A397	D398
CaSR	**S147**	**S170**	**D190**	**Q193**	**Y218**	**F270**	**S296**	**E297**
T1R1	T149	**S172**	**D192**	**Q195**	**Y220**	**F274**	**S300**	**E301**
T1R2	**S144**	I167	A187	H190	**Y215**	**F275**	**S301**	**E302**
T1R3	**S147**	**S170**	**D190**	**Q193**	**Y218**	**F274**	**S300**	**E301**

TABLE THREE

Summary of the effects of various CaSR mutations affecting residues delineating the Ca^{2+}-binding site

For WT and Q193A, F270A, S296A, E297D, and E297K mutant receptors, EC_{50} values for Ca^{2+} and maximal Ca^{2+}-induced [^{3}H]IP stimulation were calculated from response curves described in Fig. 3. The maximal stimulation by mutant receptors is expressed as a percent of that observed for the WT receptor in the same experiment. Data are means ± S.E. (2–5 independent experiments).

Receptor	Maximal response	Ca^{2+}, EC_{50}
	%	mM
WT	100 ± 2	4.3 ± 0.2
S147A[a]	47 ± 1	18.0 ± 0.4
S170A[a]	38 ± 1	23.1 ± 0.5
D190A[a]	45 ± 1	22.1 ± 0.4
Q193A	102 ± 7	7.6 ± 0.7[b]
Y218A[a]	27 ± 2	38 ± 3.2
F270A	66 ± 5[b]	6.1 ± 0.3[c]
S296A	76 ± 9[b]	5.4 ± 0.3[b]
E297D	94 ± 5	2.7 ± 0.3[b]
E297K	19 ± 2[b]	>10[b]

[a] Results are from Zhang *et al.* (23) and represent measurement of intracellular Ca^{2+} imaging. Values are normalized to the response of the WT receptor at 50 mM Ca^{2+}.
[b] $p < 0.01$ compared with the WT.
[c] $p < 0.05$.

(three amino acids instead of four) and a single-residue upward shift aligning His-413, and not Thr-412 (CaSR sequence), with Lys-409 (mGluR1 sequence). However, both residues present a side chain pointing inward toward the binding cavity and are putative anchoring residues for a ligand (Fig. 2, *B* and *C*). For the other 18 of the 19 residues lining the glutamate binding cavity, the multiple sequence alignment is unambiguous and identical to that proposed previously (3).

Our model shows that the CaSR presents a binding cavity between the two lobes of the amino-terminal domain, which is reminiscent of an amino acid-binding site but of smaller dimensions than that observed for the mGluR1 (47 *versus* 68 Å^3, respectively) (Fig. 2, *B* and *C*). More importantly, however, Ca^{2+} is not predicted to bind within this pocket homologous to the glutamate binding cavity. Rather, the Ca^{2+} binding is predicted to occur within an adjacent site formed by a set of polar residues directly involved in Ca^{2+} coordination (Ser-170, Asp-190, Gln-193, Ser-296, and Glu-297) (Fig. 2*C*) with an additional set of residues contributing to complete the coordination sphere of the cation (Phe-270, Tyr-218, and Ser-147) through water interactions. A pentagonal bipyramidal coordination of metal is proposed, as is observed in many calcium-binding proteins (32). Our present model identifies the presence of a Ca^{2+} binding pocket with the identification of Glu-193, Phe-270, Ser-296, and Glu-297 as novel potential residues involved in Ca^{2+} binding.

The residues involved in this putative Ca^{2+}-binding site are all conserved in T1R3 and all but one in T1R1 (Ser-147 in CaSR substituted by Thr-149 in T1R1) (TABLE TWO). They are also conserved in mGluRs and GPRC6a except for two residues (Ser-170 and Glu-297 in CaSR substituted by Thr and Asp, respectively, in mGluRs and GPRC6a). The lowest homology is found with T1R2 and GBR1 (TABLE TWO).

Functional Characterization of the Putative Ligand Contacting Residues—Four of the putative ligand contacting residues, Ser-147, Ser-170, Asp-190, and Tyr-218, have been shown previously to impair human CaSR activation when mutated to alanine (23) (TABLE THREE). Similar results were obtained for Ser-147 and Ser-170 for the rat CaSR (21). In addition, Tyr-218 mutations (Y218C and Y218S) have been identified in humans with familial hypocalciuric hypercalcemia (33, 34). To assess the functional importance of the remaining putative Ca^{2+}-contacting residues, we measured PI hydrolysis as a function of extracellular Ca^{2+} concentration in HEK293 cells transfected with the WT receptor and CaSR constructs harboring the naturally occurring E297D and E297K mutations or the artificial Q193A, F270A, and S296A mutations. The functional characterization of the E297D mutation identified in the family described above indicated that this receptor shows a left-shifted concentration-response curve to Ca^{2+} compared with the WT receptor (EC_{50} = 2.70 ± 0.30 mM *versus* 4.30 ± 0.20 mM, mean ± S.E., $n = 4$, $p < 0.001$) (Fig. 3*A* and TABLE TWO). In contrast, the E297K receptor was accompanied by a complete loss of Ca^{2+} sensitivity (Fig. 3*A* and TABLE THREE). The three Q193A, F270A, and S296A mutants demonstrated a right-shift in Ca^{2+} sensitivity compared with the WT receptor (Fig. 3*A* and TABLE THREE). The expression of WT and mutant receptors was demonstrated by Western blot analysis using the 141Ab antiserum directed against the carboxyl-terminal domain of the human CaSR that we have characterized recently (25) (Fig. 3*B*). Under reducing conditions, two main polypeptides of 150 and 130 kDa were identified in membrane preparations from HEK293 cells transfected with the WT or with the mutant receptors. These results are in agreement with those published by Bai *et al.* (35) showing that the polypeptide of higher molecular weight corresponds to *N*-linked glycosylated

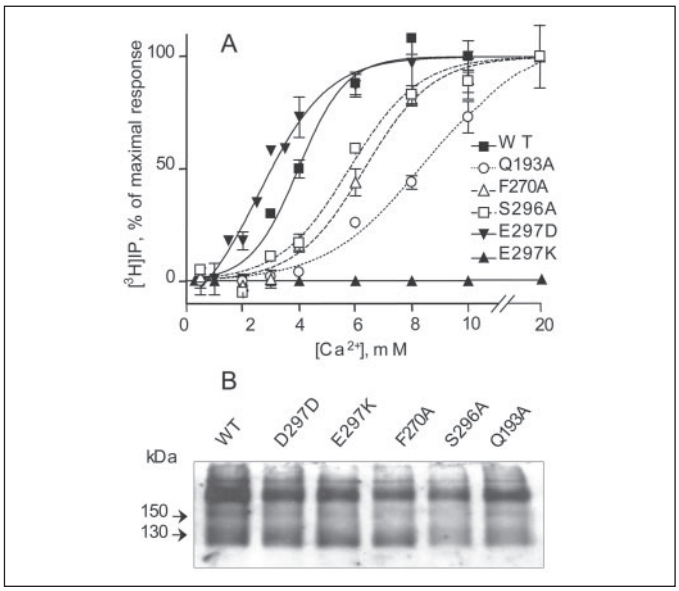

FIGURE 3. **Functional characterization and immunoblot analysis of WT and mutant CaSRs.** *A,* HEK293 cells were transfected with the WT and mutant constructs, and concentration-response curves of Ca^{2+}-induced [^{3}H]IP stimulation were performed as described under "Experimental Procedures." Data are expressed as percent of maximal response, defined as that observed following stimulation with 20 mM Ca^{2+}, and are the mean ± S.E. of triplicate determinations. The experiments were performed 2–5 times. The results shown are from a typical experiment. *B,* immunoblot analysis of whole cell lysates from HEK293 cells transfected with the WT and mutant CaSRs. Two major bands of glycosylated receptor proteins (*arrowheads*) were detected, as described previously (25).

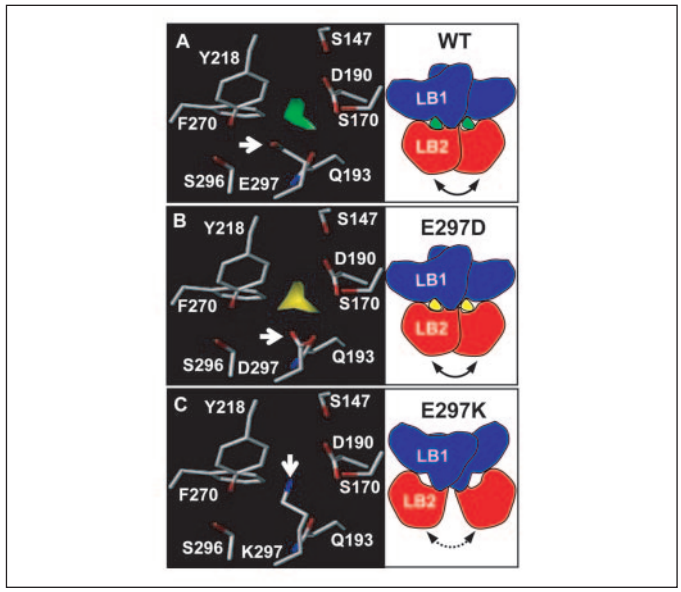

FIGURE 4. **Schematic representation of the most favorable interaction area of Ca^{2+} with WT, E297D, and E297K mutant receptors.** For the WT CaSR (*A*) and E297D mutant receptor (*B*), the most favorable interaction area (in *green* and *yellow*, respectively) is displayed at a similar interaction energy (−37.5 kcal·mol^{-1}). For the E297K mutant (*C*), the Lys-297 ammonium side chain prevents Ca^{2+} binding, and its interaction energy with amino acids located in the Ca^{2+} binding pocket is only −11 kcal·mol^{-1} and presumably not sufficient for initiating receptor activation. *White arrows* pinpoint the residue 297 side chain. *A–C, right*, diagrams of closed forms of the dimeric WT and mutant CaSR VFTMs are shown. The VFTMs are formed by two lobes (*LB1* and *LB2*) and are presented in a closed position with Ca^{2+} bound (*A* and *B*) or not (*C*) to the module. In the E297K mutant, the rotation that is thought to occur around an axis through the VFTMs dimer interface (54) presumably does not occur, thus preventing receptor activation as indicated by the *dotted arrow* in *C* and the *plain arrows* in *A* and *B*.

receptors expressed at the cell surface, whereas the lower molecular weight polypeptides represent intracellular mannose-modified receptors. In all cases, dimers migrating above 200 kDa were observed. The expression pattern of the various receptors was similar as assessed by immunoblot and was comparable with the one obtained from receptors harboring mutation at the level of the transmembrane domain and impairing recognition to calcilytics and calcimimetics (18, 25). Thus, taken together, our *in vitro* data and those from the literature (21, 23) demonstrate the importance of the eight putative ligand-contacting residues for CaSR activation. Furthermore, our data demonstrate the involvement of E297D and E297K mutations in ADH and FHH, respectively.

Analysis of the Interaction Area of Ca^{2+} with WT, E297D, and E297K CaSR—In order to understand further the effect of E297D and E297K mutation on Ca^{2+} binding, we determined the most favorable interaction area of Ca^{2+} with WT and E297D and E297K mutant receptors based on our model. For the WT and E297D mutant, the most favorable interaction area is displayed at a similar interaction energy of −37.5 kcal·mol^{-1} (Fig. 4, *A* and *B*, in *green* and *yellow*, respectively). In contrast a lower desolvation energy ($\Delta\Delta G_{desolv} = -4.53$ kcal·mol^{-1}) is required for the E297D mutant compared with the WT receptor. In the E297K mutant, the model shows that the ammonium side chain of the lysine residue exactly occupies the Ca^{2+} binding area (Fig. 4, *C*, *left*).

DISCUSSION

In the present work, we identify a set of residues delineating a Ca^{2+} binding pocket within the VFTM of the human CaSR. This binding pocket is adjacent to, but distinct from, a cavity reminiscent of an amino acid-binding site involved in amino acid recognition in mGluRs, GBR1 and GPRC6a. It is conserved within the VFTM of several class III GPCRs, thereby providing a molecular basis for the effects of Ca^{2+} on these receptors. We validate the model and provide direct clinical evidence for the physiological relevance of the VFTMs to class III GPCRs by characterizing pathogenic activating and inactivating mutations associated with a single amino acid of the CaSR located within the proposed Ca^{2+} binding pocket.

The construction of a three-dimensional model of the CaSR VFTM based on the mGluR1 crystal structure (3), and on the alignment of CaSR amino-terminal amino acid sequence with that of class III human GPCRs, allowed us to predict that the Ca^{2+}-binding site of the CaSR comprises eight residues located within the cleft of the two putative VFTM lobes. Two sets of observations validate our model. First, functional studies, as shown here and by others (21, 23), demonstrate the importance of these residues for activation of the CaSR by Ca^{2+}. Second, our model predicts that the Ca^{2+}-binding site of the CaSR is centered on the acidic residue Glu-297. We report and characterize a novel activating mutation in the CaSR in a family affected with ADH, resulting from the conservative E297D substitution. A counterpart loss of function mutation, E297K, had been reported in patients with FHH (30, 31). Most interestingly, a glutamate residue is found at the homologous position in the human T1R1, T1R2, and T1R3 (and in a set of mouse vomeronasal receptors V2R2) (36), whereas an aspartate residue is found in all mGluRs (Asp-318 and Asp-309 in mGluR1 and mGluR8, respectively), GPRC6a and GBR1. Asp-318 in mGluR1 has been demonstrated to be part of the ligand binding pocket (3), and introducing the D309E substitution in mGluR8 results in a decrease in glutamate-induced stimulation of IP production in transfected cells and in a conversion of antagonists into agonists (4). Therefore, it appears that this residue plays a pivotal role in determining ligand affinity for this family of receptors and is implicated in proper receptor activation.

With respect to the known structure of the glutamate-binding site in the mGluR1, the main distinct features of our CaSR model are observed

at the putative α-amino acid-binding site where all residues interacting with the carboxylate side chain of glutamate in mGluR1 are not conserved in CaSR (Tyr-74 to Arg-66, Arg-323 to Ser-302, and Lys-409 to His-413) (Fig. 2, *B* and *C*, and TABLE ONE). In contrast, the second part of the α-amino acid-binding site is conserved or conservatively substituted, and all residues have been shown to be ligand-binding residues in the mGluR1, with the exception of Gln-211 (Gln-193 in the CaSR) (3). The presence of Arg-66 and Ser-302 in the CaSR (replacing Tyr-74 and Arg-323 in mGluR1) would prevent the binding of acidic molecules such as glutamate. In this regard, aromatic L-amino acids such as L-phenylalanine have been proposed to potentiate the effects of Ca^{2+} on the CaSR (37). However, we have not been successful in demonstrating such modulation of the WT human CaSR response to Ca^{2+} under our standard experimental conditions (data not shown). Two residues interacting with the glutamate carboxylate main chain via a water molecule in mGluR1 have been changed in CaSR (Glu-292 to Ser-272 and Ser-164 to Gly-146). Finally, the Asp-318 (mGluR1) to Glu-297 (CaSR) substitution would disfavor the ionic interaction with the ammonium main chain moiety of an α-amino acid. It therefore appears unlikely that α-amino acids bind to the bilobal-binding site of CaSR in a manner analogous to the interaction between glutamic acid and the metabotropic receptors.

Based on our model, residues delineating the Ca^{2+}-binding site within the VFTM of the CaSR are all conserved in T1R3 and all but one conserved in T1R1. This model suggests that activation of these receptors might be also modulated by Ca^{2+}. Most interestingly, T1R3 is necessary for the functional expression of T1R1 and T1R2. T1R1/T1R3 heterodimers have been proposed to serve as L-amino acid sensors and to respond to the umami taste stimulus L-glutamate, whereas T1R2/T1R3 heterodimers have been designated as sweet receptors (38–40). These receptors have been hypothesized to be involved in sugar sensing on the tongue and possibly in other tissues such as the intestine (41) where they could be involved in a taste-sensing mechanism present in the gastrointestinal tract (42). A working model for the sweet and umami taste receptors proposes that L-glutamate and aspartame interact with the amino-terminal extracellular domain of T1R1 and T1R2, respectively (5). Further functional experiments are required to identify whether such responses are modulated by Ca^{2+}, acting either on T1R1, T1R2, T1R3, or all three heteromers.

Most interestingly, all residues predicted to be located in the close vicinity of the Ca^{2+}-binding site and whose mutations affect Ca^{2+} binding (Ser-147, Ser-170, Asp-190, Ser-296, and Glu-297), as demonstrated here (Fig. 3 and TABLE TWO) and in previous reports (21, 23), are conserved or conservatively substituted in all mGluRs and most class III GPCRs (TABLE ONE). This may explain why the activity of the related mGluRs, GBR1 and GPRC6a, are Ca^{2+}-dependent (43–45) and why this dependence is sensitive to single point mutations affecting amino acids adjacent to the Ca^{2+}-binding site (S166D for mGluR1 and S269A for GBR1) (44, 46). The effect of Ca^{2+} acting at the level of the VFTM on the GBR1 occurs at a relatively high affinity (around 40 μM) (44), whereas the activity of the CaSR is modulated by changes in the Ca^{2+} concentrations occurring in the millimolar range. Most interestingly, the mouse GPRC6a response to cysteine and histidine is potentiated by Ca^{2+} (45). These results raise the possibility that Ca^{2+} interacts with the putative Ca^{2+} binding pocket within the VFTM of various class III GPCRs with different affinities, such that the range of Ca^{2+} concentrations resulting in modulation of receptor activity would be distinct for each receptor. Such a range of Ca^{2+} concentrations is likely to be observed under pathophysiological conditions in specific tissues. Indeed, extracellular Ca^{2+} is lowered after activation of glutamate receptors in brain or following epileptic seizures (47, 48), whereas high extracellular Ca^{2+} concentrations occur in the microenvironment of bone cells. Most interestingly, the presence of an extracellular cation-sensing receptor in osteoblasts with distinct cation specificity has been identified on CaSR(−/−) osteoblasts (49, 50).

The molecular positioning of Glu-297 within the cleft of the two lobes that form the VFTM is in agreement with results obtained by the analysis of mutated receptors. Mutation of this residue in patients with ADH has not been described previously. The E297D mutation would favor the stabilization by Ca^{2+} of VFTM in the "closed" configuration necessary for receptor activation, as indicated by the lower desolvation energy for the mutated receptor compared with that of WT receptor. In contrast, in the E297K mutant associated with FHH, the Lys-297 ammonium side chain would keep the VFTMs closed by occupying the Ca^{2+} binding area, thus preventing Ca^{2+} binding. However, its interaction energy with neighboring amino acids is not sufficient to induce receptor activation.

In conclusion, we propose that the Ca^{2+}-binding site in the CaSR involves a set of polar residues directly involved in Ca^{2+} coordination (Ser-170, Asp-190, Gln-193, Ser-296, and Glu-297), and an additional set of residues that contributes to complete the coordination sphere of the cation (Phe-270, Tyr-218, and Ser-147). However, our model based on the x-ray structure of mGluR1 should be strengthened by the x-ray structure of the CaSR VFTM that has yet to be obtained. The *in vitro* demonstration in this and previous studies (21, 23) that these residues are important for the CaSR activation together with the clinical observation that the E297D and E297K mutations are responsible for ADH and FHH, respectively, are in agreement with the model. The presence of a calcium recognition site at the level of the transmembrane domains (51, 52) and of a proline residue (Pro-823) located within the putative transmembrane domain 6 playing a critical role for response to Ca^{2+} (53) suggests that, besides the VFTM, other determinants located in the seven-transmembrane domain participate in the Ca^{2+} mode of action. Our data support the physiological relevance of the VFTMs in the activation of receptors stimulated by the binding of small ligands in their extracellular domain. They are also consistent with the presence of a conserved Ca^{2+} binding pocket within class III GPCR VFTM, and thereby raise the possibility that changes in extracellular Ca^{2+} may modulate a wide range of biological responses associated with these receptors.

REFERENCES

1. Hofer, A. M., and Brown, E. M. (2003) *Nat. Rev. Mol. Cell. Biol.* **4,** 530–538
2. Pin, J. P., Kniazeff, J., Goudet, C., Bessis, A. S., Liu, J., Galvez, T., Acher, F., Rondard, P., and Prezeau, L. (2004) *Biol. Cell* **96,** 335–342
3. Kunishima, N., Shimada, Y., Tsuji, Y., Sato, T., Yamamoto, M., Kumasaka, T., Nakanishi, S., Jingami, H., and Morikawa, K. (2000) *Nature* **407,** 971–977
4. Bessis, A. S., Rondard, P., Gaven, F., Brabet, I., Triballeau, N., Prezeau, L., Acher, F., and Pin, J. P. (2002) *Proc. Natl. Acad. Sci. U. S. A.* **99,** 11097–11102
5. Xu, H., Staszewski, L., Tang, H., Adler, E., Zoller, M., and Li, X. (2004) *Proc. Natl. Acad. Sci. U. S. A.* **101,** 14258–14263
6. Liu, J., Maurel, D., Etzol, S., Brabet, I., Ansanay, H., Pin, J. P., and Rondard, P. (2004) *J. Biol. Chem.* **279,** 15824–15830
7. Wellendorph, P., Hansen, K. B., Balsgaard, A., Greenwood, J. R., Egebjerg, J., and Brauner-Osborne, H. (2005) *Mol. Pharmacol.* **67,** 589–597
8. Brown, E. M., and MacLeod, R. J. (2001) *Physiol. Rev.* **81,** 239–297
9. Hu, J., and Spiegel, A. M. (2003) *Trends Endocrinol. Metab.* **14,** 282–288
10. Brown, E. M., Gamba, G., Riccardi, D., Lombardi, M., Butters, R., Kifor, O., Sun, A., Hediger, M. A., Lytton, J., and Hebert, S. C. (1993) *Nature* **366,** 575–580
11. Ruat, M., Molliver, M. E., Snowman, A. M., and Snyder, S. H. (1995) *Proc. Natl. Acad. Sci. U. S. A.* **92,** 3161–3165
12. Garrett, J. E., Capuano, I. V., Hammerland, L. G., Hung, B. C., Brown, E. M., Hebert, S. C., Nemeth, E. F., and Fuller, F. (1995) *J. Biol. Chem.* **270,** 12919–12925
13. Riccardi, D., Park, J., Lee, W. S., Gamba, G., Brown, E. M., and Hebert, S. C. (1995) *Proc. Natl. Acad. Sci. U. S. A.* **92,** 131–135

14. Ruat, M., Snowman, A. M., Hester, L. D., and Snyder, S. H. (1996) *J. Biol. Chem.* **271,** 5972–5975
15. Chang, W. H., Pratt, S., Chen, T. H., Nemeth, E., Huang, Z. M., and Shoback, D. (1998) *J. Bone Miner. Res.* **13,** 570–580
16. Coulombe, J., Faure, H., Robin, B., and Ruat, M. (2004) *Biochem. Biophys. Res. Commun.* **323,** 1184–1190
17. Nemeth, E. F. (2002) *Curr. Pharm. Des.* **8,** 2077–2087
18. Petrel, C., Kessler, A., Dauban, P., Dodd, R. H., Rognan, D., and Ruat, M. (2004) *J. Biol. Chem.* **279,** 18990–18997
19. Block, G. A., Martin, K. J., de Francisco, A. L., Turner, S. A., Avram, M. M., Suranyi, M. G., Hercz, G., Cunningham, J., Abu-Alfa, A. K., Messa, P., Coyne, D. W., Locatelli, F., Cohen, R. M., Evenepoel, P., Moe, S. M., Fournier, A., Braun, J., McCary, L. C., Zani, V. J., Olson, K. A., Drueke, T. B., and Goodman, W. G. (2004) *N. Engl. J. Med.* **350,** 1516–1525
20. Hendy, G. N., D'Souza-Li, L., Yang, B., Canaff, L., and Cole, D. E. (2000) *Hum. Mutat.* **16,** 281–296
21. Brauner-Osborne, H., Jensen, A. A., Sheppard, P. O., O Hara, P., and Krogsgaard-Larsen, P. (1999) *J. Biol. Chem.* **274,** 18382–18386
22. Reyes-Cruz, G., Hu, J., Goldsmith, P. K., Steinbach, P. J., and Spiegel, A. M. (2001) *J. Biol. Chem.* **276,** 32145–32151
23. Zhang, Z., Qiu, W., Quinn, S. J., Conigrave, A. D., Brown, E. M., and Bai, M. (2002) *J. Biol. Chem.* **277,** 33727–33735
24. Prie, D., Huart, V., Bakouh, N., Planelles, G., Dellis, O., Gerard, B., Hulin, P., Benque-Blanchet, F., Silve, C., Grandchamp, B., and Friedlander, G. (2002) *N. Engl. J. Med.* **347,** 983–991
25. Petrel, C., Kessler, A., Maslah, F., Dauban, P., Dodd, R. H., Rognan, D., and Ruat, M. (2003) *J. Biol. Chem.* **278,** 49487–49494
26. Notredame, C., Higgins, D. G., and Heringa, J. (2000) *J. Mol. Biol.* **302,** 205–217
27. Bissantz, C., Bernard, P., Hibert, M., and Rognan, D. (2003) *Proteins* **50,** 5–25
28. Goodford, P. J. (1985) *J. Med. Chem.* **28,** 849–857
29. Kumar, S., Tamura, K., Jakobsen, I. B., and Nei, M. (2001) *Bioinformatics* **17,** 1244–1245
30. Pollak, M. R., Brown, E. M., Chou, Y. H., Hebert, S. C., Marx, S. J., Steinmann, B., Levi, T., Seidman, C. E., and Seidman, J. G. (1993) *Cell* **75,** 1297–1303
31. Bai, M., Quinn, S., Trivedi, S., Kifor, O., Pearce, S. H. S., Pollak, M. R., Krapcho, K., Hebert, S. C., and Brown, E. M. (1996) *J. Biol. Chem.* **271,** 19537–19545
32. Chattopadhyaya, R., Meador, W. E., Means, A. R., and Quiocho, F. A. (1992) *J. Mol. Biol.* **228,** 1177–1192
33. Pearce, S. H., Trump, D., Wooding, C., Besser, G. M., Chew, S. L., Grant, D. B., Heath, D. A., Hughes, I. A., Paterson, C. R., Whyte, M. P., and *et al*. (1995) *J. Clin. Investig.* **96,** 2683–2692
34. Cetani, F., Pardi, E., Borsari, S., Tonacchera, M., Morabito, E., Pinchera, A., Marcocci, C., and Dipollina, G. (2003) *Clin. Endocrinol.* **58,** 199–206
35. Bai, M., Trivedi, S., and Brown, E. M. (1998) *J. Biol. Chem.* **273,** 23605–23610
36. Mombaerts, P. (2004) *Nat. Rev. Neurosci.* **5,** 263–278
37. Conigrave, A. D., Quinn, S. J., and Brown, E. M. (2000) *Proc. Natl. Acad. Sci. U. S. A.* **97,** 4814–4819
38. Nelson, G., Hoon, M. A., Chandrashekar, J., Zhang, Y., Ryba, N. J., and Zuker, C. S. (2001) *Cell* **106,** 381–390
39. Nelson, G., Chandrashekar, J., Hoon, M. A., Feng, L., Zhao, G., Ryba, N. J., and Zuker, C. S. (2002) *Nature* **416,** 199–202
40. Li, X., Staszewski, L., Xu, H., Durick, K., Zoller, M., and Adler, E. (2002) *Proc. Natl. Acad. Sci. U. S. A.* **99,** 4692–4696
41. Wu, S. V., Rozengurt, N., Yang, M., Young, S. H., Sinnett-Smith, J., and Rozengurt, E. (2002) *Proc. Natl. Acad. Sci. U. S. A.* **99,** 2392–2397
42. Dyer, J., Salmon, K. S., Zibrik, L., and Shirazi-Beechey, S. P. (2005) *Biochem. Soc. Trans.* **33,** 302–305
43. Kubo, Y., Miyashita, T., and Murata, Y. (1998) *Science* **279,** 1722–1725
44. Galvez, T., Urwyler, S., Prezeau, L., Mosbacher, J., Joly, C., Malitschek, B., Heid, J., Brabet, I., Froestl, W., Bettler, B., Kaupmann, K., and Pin, J. P. (2000) *Mol. Pharmacol.* **57,** 419–426
45. Kuang, D., Yao, Y., Lam, J., Tsushima, R. G., and Hampson, D. R. (2005) *J. Neurochem.* **93,** 383–391
46. Abe, H., Tateyama, M., and Kubo, Y. (2003) *FEBS Lett.* **545,** 233–238
47. Pumain, R., Kurcewicz, I., and Louvel, J. (1983) *Science* **222,** 177–179
48. Pumain, R., Kurcewicz, I., and Louvel, J. (1987) *Can. J. Physiol. Pharmacol.* **65,** 1067–1077
49. Pi, M., Garner, S. C., Flannery, P., Spurney, R. F., and Quarles, L. D. (2000) *J. Biol. Chem.* **275,** 3256–3263
50. Pi, M., and Quarles, L. D. (2004) *J. Bone Miner. Res.* **19,** 862–869
51. Ray, K., and Northup, J. (2002) *J. Biol. Chem.* **277,** 18908–18913
52. Hu, J., Reyes-Cruz, G., Chen, W., Jacobson, K. A., and Spiegel, A. M. (2002) *J. Biol. Chem.* **277,** 46622–46631
53. Hu, J., McLarnon, S. J., Mora, S., Jiang, J., Thomas, C., Jacobson, K. A., and Spiegel, A. M. (2005) *J. Biol. Chem.* **280,** 5113–5120
54. Hu, J., Mora, S., Colussi, G., Proverbio, M. C., Jones, K. A., Bolzoni, L., De Ferrari, M. E., Civati, G., and Spiegel, A. M. (2002) *J. Bone Miner. Res.* **17,** 1461–1469